General method for thickness determination of thin backed films. New formulation of backscattering spectrometry

E.F. AGUILERA, E. MARTÍNEZ-QUIROZ,
H.M. BERDEJO AND M.C. FERNÁNDEZ
Departamento de Aceleradores, Instituto Nacional de Investigaciones Nucleares
Apartado postal 18–1027, 11801 México, D.F., México

Recibido el 27 de febrero de 1995; aceptado el 18 de abril de 1995

ABSTRACT. On the basis of the global energy change of particles going through a film, which are backscattered from the surface of the film backing, a general method is described to determine the thickness of thin films deposited on thick substrates. Using a range formulation of the process, three analytic approximations and a quite fast computer program to calculate the exact value are developed. Supporting measurements are performed on 14 targets using carbon beams. For the particular situation of a substrate with a heavier atomic mass than the film, precisions on the order of 1% can be obtained if uncertainties in the range data are disregarded. Comparison with other methods which are either much more complex, or of more limited applicability, gives consistent results.

RESUMEN. Con base en el cambio global de energía de las partículas que al atravesar una película son retrodispersadas por la superficie del sustrato, se describe un método general para determinar el grosor de películas delgadas depositadas sobre sustratos gruesos. Usando una formulación del proceso en términos de alcances, se desarrollan tres aproximaciones analíticas y un programa rápido de cómputo para calcular el valor exacto. Se realizan mediciones de respaldo en 14 blancos usando haces de carbón. Para la situación particular de un sustrato con mayor masa atómica que la película, se pueden obtener precisiones del orden de 1% si se descartan las incertidumbres en los datos de alcance. La comparación con otros métodos que son, o más complejos o de una aplicabilidad más limitada, arroja resultados consistentes.

PACS: 29.25

1. INTRODUCTION

The determination of the thickness of thin foils is important in several areas of physics. In experimental nuclear physics, for example, the target thickness is necessary to obtain absolute values of the experimental cross sections for a given nuclear reaction. Taking advantage of the fact that both the kinematics of elastic scattering and the energy loss of charged particles in the interaction with matter are sufficiently well known processes, some techniques based on these processes have been routinely used to determine target thicknesses. For a transmission target, for example, the thickness can be determined by measuring the energy loss of transmitted particles and comparing it with the energy loss calculated from known data of dE/dx as a function of energy. On the other hand, when the

target is a film deposited on a thick substrate made out of an element lighter than the film itself, the thickness can be determined by detecting the backscattered particles [1–3]. In this case, a peak separated from the thick-target background is obtained in the backscattering spectrum whose width is directly correlated to the film thickness since the high energy edge of the peak is generated by particles backscattered from atoms at the front surface of the film, while the low energy edge corresponds to particles backscattered from the film atoms at the rear. This technique can be also applied to transmission targets, of course.

The analytical methods of backscattering spectrometry have been traditionally based upon a stopping-power formulation, in the sense that the formulas used to calculate the energy loss of a projectile that has penetrated some depth x into a target, are always expressed in terms of the corresponding stopping powers dE/dx. This implies that the calculations do in general involve energy integrations, and thus it should be easier to perform them using range values rather than stopping powers because the ranges are actually integrated path lengths and are therefore more directly related to energy losses. This motivated us to investigate a formulation of backscattering spectrometry in terms of ranges, which we present in this work. The formulation is applied to a general method for thickness determination of thin films deposited on thick substrates.

When a light-element film is deposited on a heavier-element substrate, the scattering peak corresponding to the film overlaps, in the backscattering spectrum, with the background of particles scattered from the thick substrate, thus introducing cumbersome error sources in the analysis or, in some cases, making it impossible to resolve the peak.

Much interest exists on this last kind of targets. When measuring γ–rays in nuclear physics, for example, a substrate with a high atomic number such as gold or lead is very useful to stop the reaction products without producing undesirable nuclear reactions, thus effectively controlling possible Doppler shift effects in the measured γ–rays [4]. In the Doppler shift attenuation method of measuring nuclear lifetimes [5], for instance, thin films deposited on heavy-metal backings of Ni, Ta or Au are frequently used. The importance of a careful determination of the target thickness for this method has been emphasized [5]. The gamma-ray technique for measuring fusion cross sections uses also this kind of targets [6,7] and the corresponding absolute normalizations require, at some point, precise thickness determinations.

High resolution techniques have been developed for depth microscopy using elastic recoil detection analysis (ERDA) [8], but they are meant for finer applications than simple thickness determinations of elemental films and use fairly sophisticated equipment which is not available in most laboratories. To obtain depth profile information about low–Z atoms on the surface of higher–Z substrates, positive Q–value nuclear reactions such as (d,p), (d,α) and (p,α) are often used [9,10]. For low bombarding energies, where Rutherford scattering occurs, computer programs have been developed to calculate backscattering spectra [11] by doing an appropriate simulation of the involved processes. While this provides a general technique for target thickness determinations, it is rather meant for the analysis of complex samples and the many parameters involved make it somehow cumbersome for simple applications.

In the method presented here, the common techniques of backscattering spectrometry are used to determine the thickness of low–Z films on higher–Z substrates. Instead of using

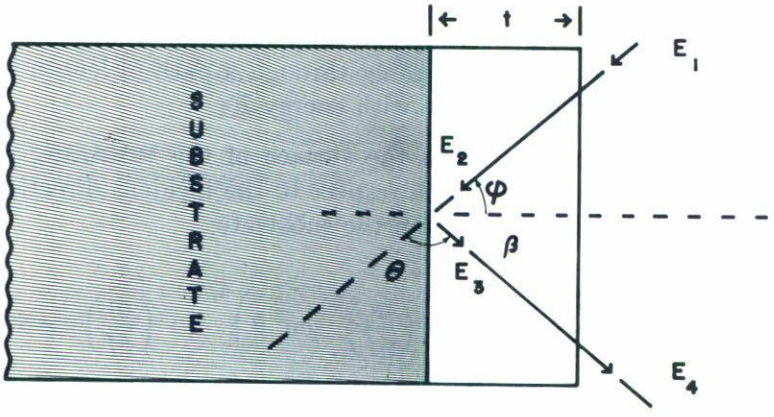

FIGURE 1. Schematic representation of ion backscattering from a substrate behind a film of thickness t.

backscattered particles from film atoms at the front and rear surfaces, the method compares the energies of backscattered particles from substrate atoms in the two situations in which a bare substrate or a substrate with film is bombarded. With this method, the thickness of a thin film deposited on a thick substrate can be determined independently of the atomic masses of film and substrate. In order to indorse the method, several experimental measurements of C, Al and Ag targets on Ta substrates are presented. For the case of the Ag target, additional substrates of Al and Fe are analyzed. Although the method is formulated for a general projectile, the experiments are performed with a heavy ion instead of the usual He beam because of availability limitations in our laboratory. We notice, however, that an improved depth resolution has been claimed for heavy ions in the literature [12].

The formulation of the method is introduced in Sect. 2 and discussed in Sect. 3. In Sect. 4, the experimental details and the method of analysis are described. The experimental results and a comparison with other methods or other types of analysis are presented in Sect. 5. Finally, some concluding remarks are given in Sect. 6.

2. THEORETICAL ASPECT OF THE METHOD

When a projectile interacts with some medium, its energy can be changed because of different effects. The interaction with atomic electrons produces a gradual energy loss which is an increasing function of the penetrated depth. The scattering by nuclei of the material, on the other hand, causes a sudden energy change of the projectile. The present method is based upon measurements of the total energy change of backscattered particles with respect to incident projectiles because of these two effects.

Figure 1 shows schematically the process of backscattering of a projectile from a substrate-film combination in which the film has thickness t. We emphasize that in this figure we mean to represent backscattering from substrate atoms rather than from film atoms at the interface. In this geometry the incident beam, the normal to the target surface and the outgoing particles are all assumed to be in the same plane. On the basis of the above mentioned effects, this process can be divided in three stages:

1) A projectile with energy E_1 penetrates the target making an angle φ with respect to the normal to the surface and, after going through a path of length $t_1 = t/\cos\varphi$, it arrives at the surface of the substrate with energy E_2.

2) The projectile is backscattered from the surface of the substrate, going out with energy $E_3 = K_s E_2$, at an angle θ with respect to the incident direction, where K_s is the kinematic factor for scattering from the substrate:

$$K_s = \left(1 + \frac{m}{M}\right)^{-2} \left[\left(1 - \left(\frac{m}{M}\right)^2 \operatorname{sen}^2\theta\right)^{1/2} + \left(\frac{m}{M}\right)\cos\theta\right]^2 ; \tag{1}$$

here m and M are the atomic masses of the projectile and the substrate, respectively.

3) After traversing back the target, going through a path of length $t_2 = t/\cos\beta$, the backscattered particle leaves the target with energy E_4.

In order to determine the film thickness from the known experimental quantities, we will assume that the range $R(E)$ of the projectile in the given film can be determined for any value of the energy E. The published tables of $R(E)$, together with appropriate interpolations, are enough for our purposes. The lengths of the ingoing and outgoing paths can then be expressed as

$$\frac{t}{\cos\varphi} = R(E_1) - R(E_2), \tag{2}$$

$$-\frac{t}{\cos(\theta + \varphi)} = R(K_s E_2) - R(E_4). \tag{3}$$

Notice that the usual formulation uses the equivalent integral expressions of the form $\int dE/(dE/dx)$, with appropriate limits, instead of the simple differences in the right-hand-side of Eqs. (2) and (3). E_2 has to be eliminated from these two equations in order to solve them for t. We shall consider first some approximations that will allow us to find analytic expressions for t and then we will see how an exact numerical solution can be found.

2.1. Linear approximation

If we assume that, for E between E_4 and E_1, $R(E)$ can be approximated by a straight line,

$$R(E) = aE + b, \tag{4}$$

it is easy to eliminate E_2 from Eqs. (2) and (3) to find

$$t = \frac{a(K_s E_1 - E_4)}{\dfrac{K_s}{\cos\varphi} - \dfrac{1}{\cos(\theta + \varphi)}}, \tag{5}$$

where the slope, a, can be calculated from

$$a = \frac{R(E_1) - R(E_4)}{(E_1 - E_4)}. \tag{6}$$

In the language of stopping powers, the linear approximation may be stated as $dE/dx = \text{constant} = a^{-1}$, where the constant a is given by Eq. (6).

2.2. Piecewise linear approximation

Noticing, from simple physical arguments, that $E_4 < E_3 < K_s E_1$ and $E_4/K_s < E_2 < E_1$, the linear approximation can be improved by assuming different straight line behaviours for $R(E)$ in the two regions defined by the above inequalities. The new expression for t is then

$$t = \frac{(K_s E_1 - E_4)}{\dfrac{K_s}{a_1 \cos\varphi} - \dfrac{1}{a_2 \cos(\theta + \varphi)}}, \tag{7}$$

where the slopes, a_1 and a_2, are given by

$$a_1 = \frac{R(E_1) - R(E_4/K_s)}{(E_1 - E_4/K_s)}, \qquad a_2 = \frac{R(K_s E_1) - R(E_4)}{(K_s E_1 - E_4)}. \tag{8}$$

The basic assumption in this approximation corresponds to using different constant values, a_1^{-1} and a_2^{-1}, for dE/dx along the inward and outward paths, respectively. This is the same assumption underlying the standard surface energy and mean energy approximations, where the denominator in Eq. (7) is often referred to as the backscattering energy loss factor or S factor [1,3]. The expressions obtained here for a_1 and a_2 [Eq. (8)] differ, however, from those given in the standard approximations. In the mean energy approximation, for example, an extra physical assumption to estimate the energy E_2 before scattering has to be made.

An additional analytic expression for t can be obtained in a straightforward way within our approach by replacing the two straight lines in the piecewise liner approximation by two parabolas that can be obtained from appropriate fits to the range data. Because the resulting expression is fairly long, and since the exact solution will be discussed next, it is not worthwhile to present it here, but some illustrative calculations using this piecewise parabolic approximation will be shown later in Fig. 4.

2.3. Exact solution

If for any given value of the range, the corresponding value of the energy for which the projectile has that range can be found, E_2 can be eliminated from Eqs. (2) and (3) to give a general equation for t:

$$R\left(K_s R^{-1}\left(R(E_1) - \frac{t}{\cos\varphi}\right)\right) + \frac{t}{\cos(\theta + \varphi)} - R(E_4) = 0, \tag{9}$$

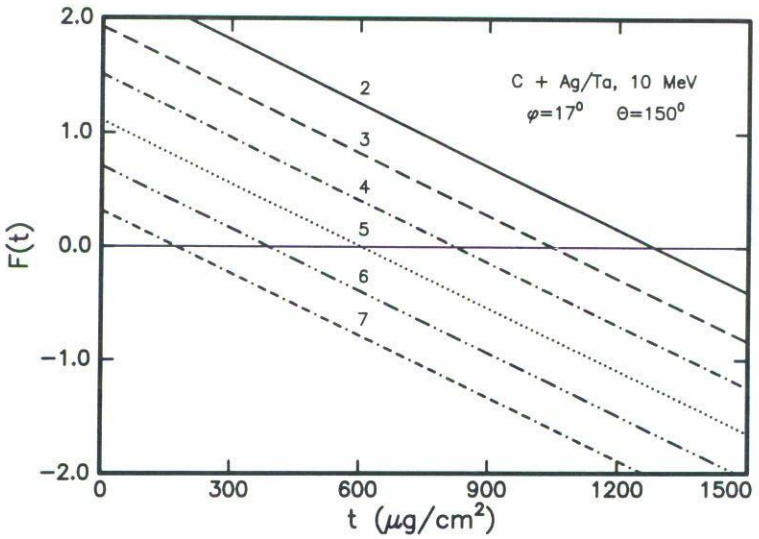

FIGURE 2. Plots of $F(t)$ vs t, where $F(t)$ is the left-hand-side of Eq. (9). The corresponding values of E_4 (MeV) are indicated above each curve.

where R^{-1} denotes the inverse function of R. Because of the typically slow change of slope of the $R(E)$ curves in the regions of interest, the left-hand-side of Eq. (9) varies nearly linearly with t around its root. This is illustrated in Fig. 2, where the values reported by Northcliffe and Schilling [13] were used for the ranges, along with a cubic spline interpolation.

The solution to Eq. (9) can thus be easily found using the method of the secant, where the root is approached by tracing secants through successive pairs of points [14]. The two starting points used to initialize the method can be taken from the approximations (5) and (7), respectively. With this procedure, two iterations are usually enough to obtain the root with an accuracy better than 10^{-6} %, typically involving a computer time of less than 3 milliseconds at a HP Apollo 730 workstation (actually, one single iteration is usually enough to obtain the result, but the program makes a second iteration to assure that convergence has been reached).

The experimental error in this method is calculated from the following formula:

$$\Delta t = \left[\left(\frac{\partial t}{\partial E_4} \right)^2 (\Delta E_4)^2 + \left(\frac{\partial t}{\partial \varphi} \right)^2 (\Delta \varphi)^2 + \left(\frac{\partial t}{\partial \theta} \right)^2 (\Delta \theta)^2 \right]^{1/2} \tag{10}$$

We must emphasize that the inaccuracies present in the range data are not taken into account in this expression and they should be convoluted with Δt in order to obtain the total error. With the purpose of saving lengthy numerical calculations, the expression for t given in Eq. (7) can be used to evaluate the partial derivatives appearing in Δt if the approximation of negligible variation of a_1 and a_2 with E_4 and θ is made. A comparison with exact numerical calculations for many typical cases, using for the derivatives a three point formula and Richardson extrapolation [14], gave maximum differences in the derivatives of the

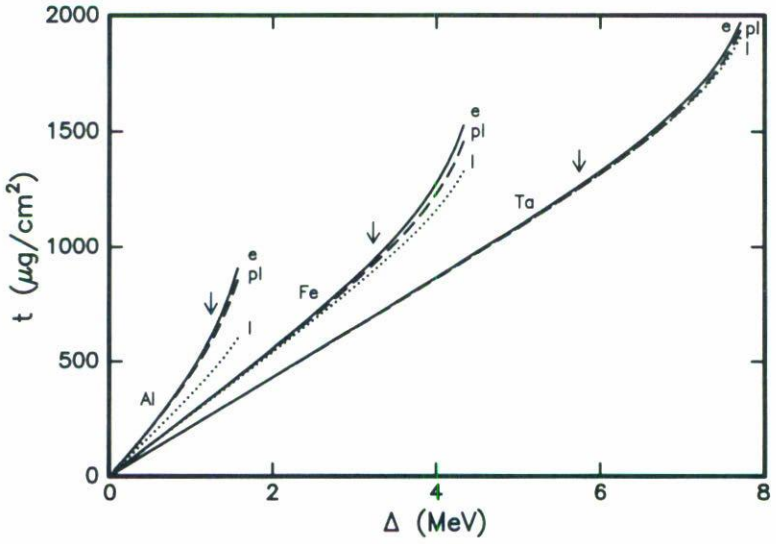

FIGURE 3. Curves of film thickness vs Δ, where $\Delta = K_s E_1 - E_4$, as calculated from the linear (l), the piecewise linear (pl) and the exact expression (e). Carbon projectiles of 10 MeV ($\theta = 150°$, $\varphi = 20°$) and Ag films on Al, Fe and Ta substrates are assumed here. The arrows indicate the limit of maximum accesible depth.

order of 0.1%. The value of the ratio $\Delta t/t$ obtained with this procedure can then be used to calculate the experimental error by simply taking its product with the exact value of t.

3. DISCUSSION

3.1. Comparison of approximations with exact calculations

Rather than E_4, the difference $\Delta = K_s E_1 - E_4$ is more directly related to the target thickness, since it actually measures the energy lost in the target. Experimentally, $K_s E_1$ corresponds to the edge of the bare-substrate spectrum while E_4 corresponds to the edge of the target-plus-substrate spectrum, so that Δ is actually the experimentally determined quantity. These are the reasons why it is preferred to present the results in terms of Δ rather than E_4.

Figure 3 shows some examples of curves of t as a function of Δ as calculated from the linear, the piecewise linear and the exact expression. Carbon projectiles of 10 MeV and Ag targets on Al, Fe and Ta substrates are assumed in these calculations. The curves are terminated at a maximum values of $\Delta = K_s E_1$, corresponding to $E_4 = 0$ for each case, although the experimentally accessible depth imposes a lower bound for Δ since E_4 must be large enough for the particle to be detected. Following Ref. [1], the conditions of accessible depth can be taken as $E_4 \geq K_s E_1/4$, or $\Delta \leq (3/4) K_s E_1$, which is indicated by the arrows in Fig. 3.

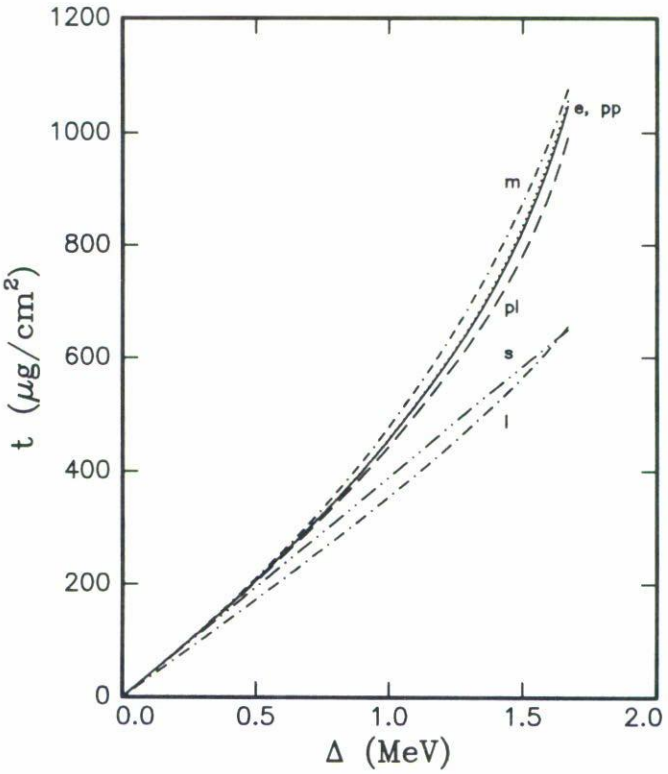

FIGURE 4. Same as Fig. 3 for the Al-substrate case. Results obtained with the surface energy (s), the mean energy (m), and the piecewise parabolic (pp, dots) approximations are included here.

We can see from Fig. 3 that the piecewise linear assumption gives always a better approximation than the simple linear one, as expected. They both give a good approximation for the case of the heavier substrate in the whole range of accessible depths, giving essentially the same value within this range with a maximum error, with respect to the exact calculation of less than 0.8%. For the lighter substrate, where K_s is much smaller, the difference between E_1 and E_4 is so large that the range curve within these values is very far from a single straight line and the linear approximation fails badly. The piecewise linear approximation, however, is still a good approximation for this case within the range of accessible depths. The maximum errors of the two approximations in this range are 3.4% and 24.7%, respectively. An intermediate situation is obtained for the medium-mass substrate, where the errors of the two approximations at the maximum accesible depth are 2.0% and 5.1%, respectively.

In order to compare with the standard approximations we picked the Al-substrate case of Fig. 3, which is the worst case in terms of our approximations, and made calculations using the surface energy and the symmetrical mean energy approximations [1], as well as the piecewise parabolic approximation mentioned earlier. The results are presented in Fig. 4, where we see that our piecewise linear approximation is similar in accuracy to the mean energy approximation and therefore much better than the surface energy one. The piecewise parabolic approximation, on the other hand, is the best one with a maximum error of less than 1% with respect to the exact calculation for this rather unfavourable case.

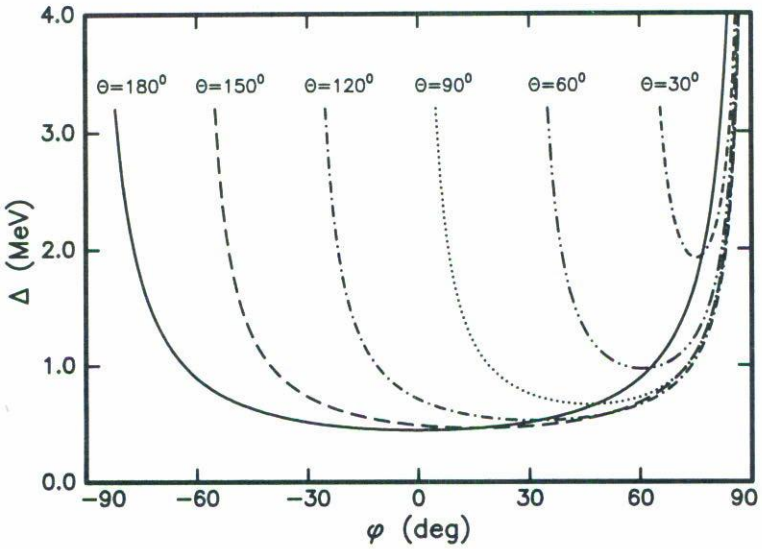

FIGURE 5. Plots of Δ vs φ for different values of θ, where $\Delta = K_s E_1 - E_4$. The calculations, obtained from solving Eq. (9), correspond to a target of 100 μg of Ag on a Ta substrate, and a carbon beam of 10 MeV.

3.2. Choice of θ and φ

In principle, the only limitation upon the angles θ, φ is given by the non-grazing condition of incident and outgoing particles, *i.e.*, $0 < \theta \leq 180°$ and $90° - \theta < \varphi < 90°$, where a negative value of φ means an opposite inclination, between the surface normal and the incident direction, to that displayed in Fig. 1. In practice, however, these angles should be chosen in such a way that a small variation of any of them shall not produce large changes in Δ, the experimentally determined quantity.

Figure 5 shows an example, for a specific case, of the behaviour of Δ as a function of φ for different values of θ. We see that by choosing a large value of θ we have more freedom in the choice of φ, since the flat parts of the curves are wider for large θ. Figure 6, on the other hand, shows the behaviour of Δ as a function of θ for different values of φ. The same physical case used in Fig. 5 was calculated here. The curves with a longer flat region correspond in this case ot φ around 60°. A good choice of the pair (θ, φ) should fall in a flat region of the corresponding curves in both, Figs. 5 and 6. So, for example, $(180°, 0°)$ or $(120°, 40°)$ would be good choices for this case.

If the value of θ is fixed by some experimental condition or any other reason, a guide to choose the optimum value of φ can be found from the condition that the partial derivative of Δ with respect to φ should vanish. For a situation where the linear approximation is expected to be good, such as the case of a heavy substrate, this condition reduces to a simple equation depending only on the ratio of atomic masses of projectile and substrate, independent of the target or the bombarding energy:

$$K_s \sin(\varphi)\cos^2(\theta + \varphi) - \sin(\theta + \varphi)\cos^2(\varphi) = 0. \tag{11}$$

The solution of this equation for φ as a function of θ, obtained numerically, is given in Fig. 7 for carbon projectiles and Ta substrates. The results are essentially the same for

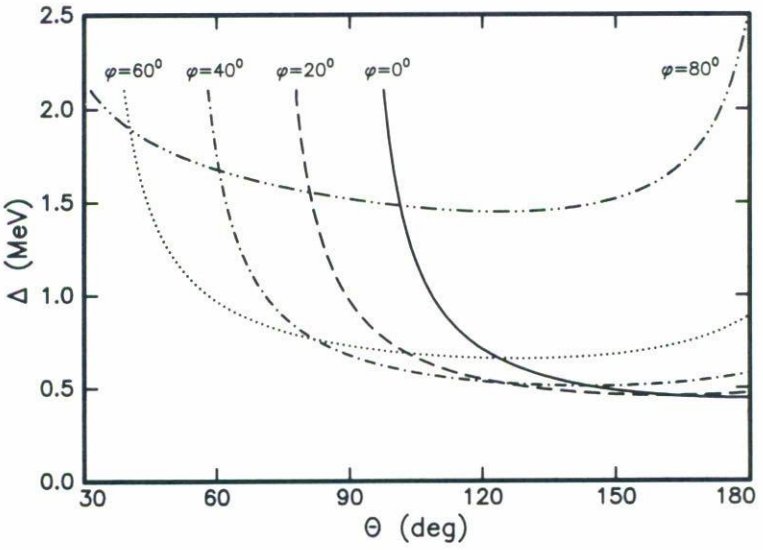

FIGURE 6. Same as Fig. 5, but Δ is plotted versus θ for different values of φ.

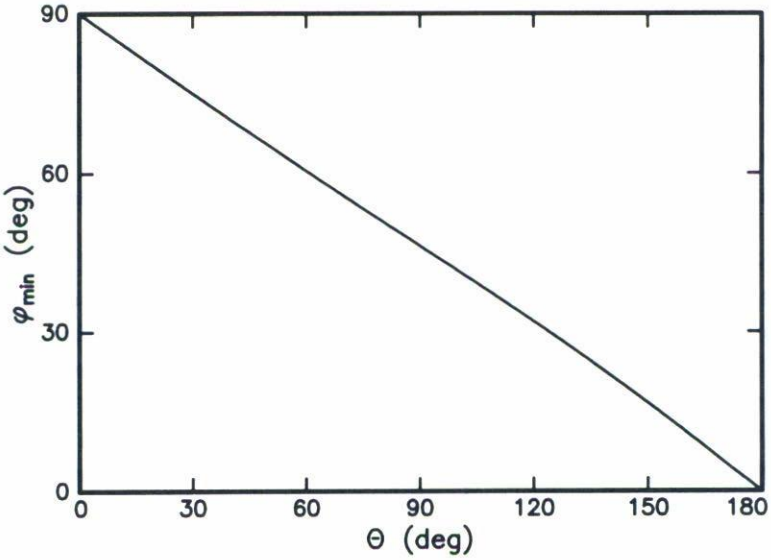

FIGURE 7. $\varphi_{\min}$ vs θ where $\varphi_{\min}$ is the solution to Eq. (11). A Ta substrate and carbon projectiles were used to calculate this curve.

heavier substrates. We can see that these results closely follow the line $\varphi = (180 - \theta)/2$, which corresponds to placing the target-normal half way between the incident and the outgoing directions. According to the previous disscusion, this provides only a guide for choosing φ and should be taken with due reserves.

4. EXPERIMENTAL DETAILS AND ANALYSIS

For implementation of the method, and with the purpose of analyzing its applicability to different situations, 14 targets were prepared with different combinations film/substrate and different amounts of material deposited on the substrate. Such combinations were: carbon deposited on tantalum, C/Ta (one target); aluminum deposited on tantalum Al/Ta (four targets); silver deposited on aluminum, Ag/Al (three targets), on iron, Ag/Fe (three targets) and tantalum, Ag/Ta (three targets).

To prepare the target of C/Ta, a thin foil of carbon was used with a nominal thickness of 5 $\mu g/cm^2$ ($\pm 20\%$). The aluminum and silver were deposited on the corresponding substrates by using the technique of high vacuum ($\sim 2 \times 10^{-6}$ torr) evaporation. For each evaporation, the several substrates were placed at different distances from the evaporation source in order to obtain targets with different thicknesses.

A 10 MeV carbon beam, obtained with the EN Tandem Van de Graaff accelerator at ININ, was used to bombard the targets, and the scattered particles were detected by three silicon surface barrier (SSB) detectors at θ values of 85°, 120° and 150°, respectively. Target inclinations of $\varphi = 40°$ or $\varphi = 52°$ were used in the measurements. In order to check the reproducibility of the method, some targets were bombarded more than once, for example on different days and setting the same experimental conditions up from scratch.

As mentioned before, the energy $K_s E_1$ corresponds to the edge of the bare-substrate spectrum, while E_4 corresponds to the edge of the target-plus-substrate spectrum. Because of system resolution and/or energy straggling in the target, these edges have the form of error functions [1] and the true positions of those energies are given by the half-height points of the edges in the corresponding spectra. In order to use the information of all neighboring points, in the present work this point was determined as the position of the maximum of the peak that results from derivation of the edge of the spectrum. This procedure was cross checked by fitting an error function to the edge, which gave the same results.

Figure 8 shows some spectra of particles backscattered on targets of Al/Ta and plain Ta, including the respective peaks obtained from derivation. A careful observation shows that the maximum of the peak corresponds always to the same relative position in the edge of the spectrum with respect to the maximum height, which confirms the reliability of our procedure.

The energy calibration was obtained from the bare-substrate spectra for the different substrates used in this work and from the high energy edge of the peaks corresponding to scattering from silver (see Fig. 9, for example). The energy loss of the particles in the gold window of the SSB detectors was corrected for in this procedure. It is worth mentioning that possible systematic errors which could be produced by calibration errors are minimized here since only the relative position of E_4 with respect to $K_s E_1$, a calibration point, is relevant in the method. Remember that both, E_4 and $K_s E_1$ are related to the experimental spectra in exactly the same way, so that by using the same criterion for determining both points in the respective spectra, a quite reliable value for the corresponding difference is obtained.

The error given by the method for each individual point was calculated in the way described at the end of Section 2, without taking into account the uncertainties in the range data. The possible effects of these uncertainties will be later discussed in terms of

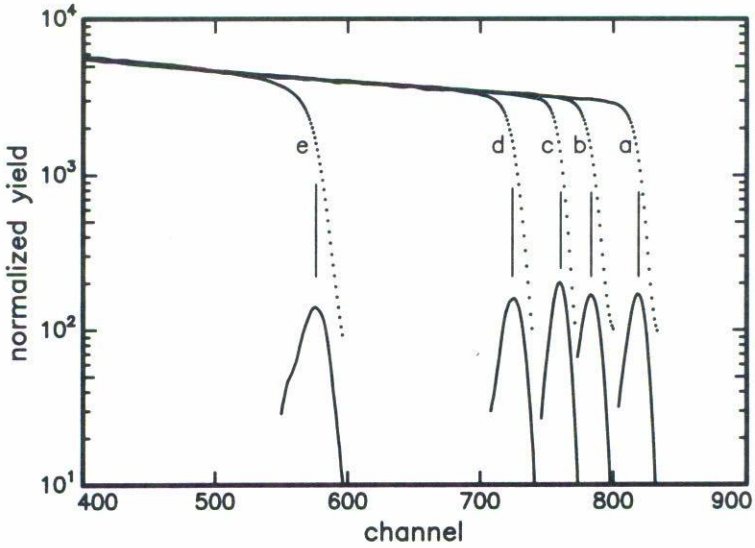

FIGURE 8. Spectra of 10 MeV Carbon projectiles scattered at $\theta = 120°$ on Al/Ta targets placed at $\varphi = 40°$. Also shown are the associated peaks resulting from the respective derivation and the positions of the corresponding maxima (vertical lines). The target thicknesses, in $\mu g/cm^2$, are: a) 0.0 (bare substrate), b) 35.8, c) 59.3, d) 93.0, and e) 236.5.

the differences obtained from a few cases in which different range tables are used. The uncertainties in θ and φ were always taken as 0.5°, while the uncertainties in E_4 were in each case related to the quality of the least squares fit to the corresponding calibration points and fluctuated around 15 keV.

5. RESULTS

The values of film thicknesses obtained with our method for all considered film/substrate combinations are presented in Table I. These values correspond to an average calculated over all measurements with the same target, including repeat points and measurements using different combinations of angles θ, φ. The reported errors are the estimated uncertainties of the mean calculated under the assumption of either equal or unequal uncertainties of the individual data points, whichever assumption gave the larger error. For about 36% of the cases, the equal uncertainties assumption gave a larger error (by a small margin), indicating the presence of some error source not included in Eq. (10), most probably related to gain drifts in the associated amplifiers.

We see from the last column of the table that the percentage errors are larger for lighter substrates, a result that can be ascribed to the fact that the steeper slopes of the corresponding curves in Fig. 3 produce larger errors in t for a given experimental error in Δ. As a consequence of the finite depth resolution of the method, the percentage errors are also larger for thinner films with the same substrate, as can be seen from the table. For the heaviest substrate, experimental errors of around 1% were typically obtained, except for the thinnest film measured.

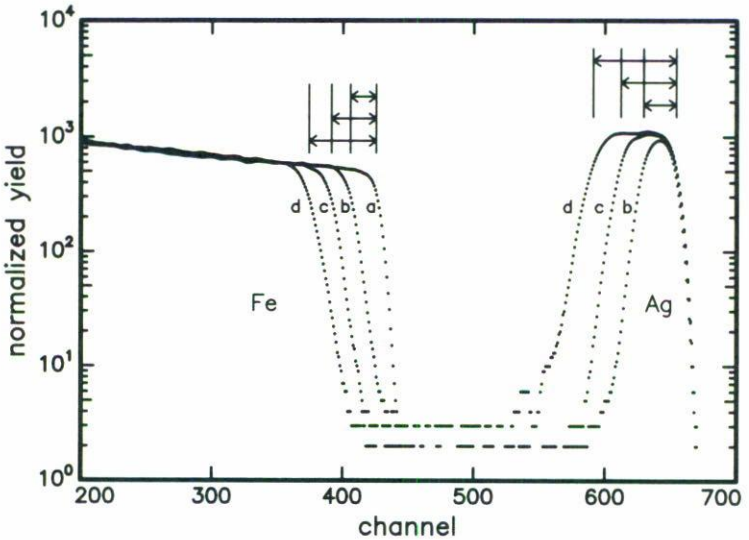

FIGURE 9. Same as Fig. 8, for Ag/Fe targets with $\theta = 150°$ and $\varphi = 40°$. For these spectra the film thickness was calculated: 1. from the relative displacement, with respect to spectrum a, of the thick target part in the left hand side, or 2. from the corresponding width of the peak in the right hand side. The corresponding thicknesses ($\mu g/cm^2$) were: a) 0.0 (bare substrate), b) 52.2, c) 88.2, and d) 135.9.

In order to get more insight into the method, three additional types of analysis were made of some of our data. In the first case, the same method was applied but the tables of ranges reported by Ziegler *et al.* [15] were used with the purpose of determining the effect of using different —but acceptable— values for the ranges. In the second case, the thicknesses were determined by doing a dynamic simulation of the complete spectra using the program RUMP [11], which uses Rutherford cross sections to calculate backscattering spectra. Since the bombarding energy in our experiments was always below the Coulomb barrier, this is a valid procedure. Finally, a determination of the thickness based on the width of the peak corresponding to scattering from the film was done for the Ag/Al and the Ag/Fe targets, where this peak is not overlapped with the thick-target background arising from the substrate.

In Table II, a comparison of the results is made for selected cases, including calculations with the piecewise linear approximation. Column 1 contains the combination film/substrate and columns 2 to 6 show the thickness obtained in five different ways. The errors obtained for the values in columns 3 and 4 (not reported) are the same as the corresponding errors in column 2. For the case of the results in columns 5 and 6, on the other hand, no uncertainty estimation was made.

For all considered cases, the piecewise linear approximation gives essentially the exact values, as shown in columns 2 and 3 of the table. In the worst case, corresponding to the thickest Ag/Al target, it agrees within 1% with the exact value, being well inside the experimental error bars. As previously discussed in section 3.1, a similar situation might be expected for any case of practical interest.

From a comparison of columns 2 and 4 of the table, it can be seen that systematically

TABLE I. Experimental values of the thickness obtained for all films analyzed in this work. t is the mean value obtained after n measurements. The corresponding percentage error is given in the last column.

film/substrate	n	t (μg/cm^2)	Δt (%)
C/Ta	2	2.5 ± 0.5	7.7
Al/Ta	2	236.5 ± 2.4	1.0
	5	93.0 ± 1.1	1.2
	2	59.3 ± 0.8	1.3
	2	35.8 ± 0.7	2.0
Ag/Al	2	167.7 ± 4.9	2.9
	3	91.7 ± 3.7	4.0
	3	52.8 ± 4.8	9.1
Ag/Fe	4	135.6 ± 2.6	1.9
	4	89.3 ± 1.8	2.0
	6	53.1 ± 1.4	2.6
Ag/Ta	4	163.2 ± 1.2	0.7
	5	96.1 ± 0.8	0.8
	7	52.0 ± 0.9	1.7

smaller thicknesses are obtained when the ranges of Ref. [15], instead of those of Ref. [13], are used in the calculation (except for the C target, discussed below). The differences are larger for lighter substrates because the energy region spanned by the projectile, $E_1 - E_4$, is larger in this case and thus the range differences for individual energies are accumulated over a longer interval. For the worst case, corresponding to the Ag/Al targets, the differences are within 4% even though the range tables present differences of up to 17% in that region. This can be understood from the fact that it is the slope, rather than the absolute values of the ranges, what is really relevant in the method (see Eqs. (7) and (8), for example) and we can therefore conclude that the effects of uncertainties in the range tables are usually minimized in this method. The exception is when the corresponding slopes are very different, as it was the case for the C/Ta target, where the energy region of interest included a crossing point of the two range curves. For the most interesting case of heavy substrates and for similar slopes of the range curves, differences of less than 1% are obtained between the two calculations, as seen from the results for the Al/Ta and Ag/Ta targets in Table II. Of course, this does not exclude the possibility of having larger differences for other materials.

As for the results obtained from RUMP calculations, presented in column 5 of Table II, they should in principle be compared with the corresponding values of column 4 since the formulas of Ref. [15] are used for energy loss in these calculations. Although the RUMP values tend to be larger than those of column 4, we can say that both calculations give fairly consistent results if the present experimental errors are considered. Further discussion of the observed differences would require a more detailed analysis of the processes involved in RUMP calculations, which is beyond the scope of this work.

TABLE II. Comparison of film thicknesses obtained from different analysis of the same spectra for some selected cases. A: present work, exact value using ranges of Ref. [13]. B: present work, pl approximation using ranges of Ref. [13]. C: present work, exact value using ranges of Ref. [15]. D: values obtained with RUMP (Ref. [11]). E: values obtained from the width of the scattering peak.

	t (μg/cm^2)				
film/substrate	A	B	C	D	E
C/Ta	6.5 ± 0.7	6.5	7.3	8.2	
Al/Ta	238.9 ± 1.4	238.6	238.2	236.3	
	91.7 ± 0.8	91.7	91.1	89.8	
	59.3 ± 1.0	59.3	59.0	58.7	
	35.8 ± 1.1	35.8	35.7	36.2	
Ag/Al	167.7 ± 5.6	166.1	163.2	171.2	175.3
	93.0 ± 6.9	92.5	88.9	90.0	96.0
	46.3 ± 6.7	46.2	44.5	48.7	52.0
Ag/Fe	138.0 ± 3.3	137.7	131.1	129.8	130.3
	88.2 ± 2.6	88.1	83.7	83.8	85.8
	52.2 ± 2.6	52.2	49.8	49.0	52.5
Ag/Ta	163.6 ± 2.2	163.6	161.1	164.9	
	97.3 ± 1.8	97.3	96.5	96.8	
	52.8 ± 1.5	52.8	52.4	54.4	

For the last type of analysis, the width of the scattering peak in spectra like those presented in Fig. 9 had to be determined. Since the system resolution was in most cases comparable to the energy lost in the target, the method described in Appendix C of Ref. [1] was used to determine this width. For the examples of Fig. 9, the widths are indicated by the horizontal arrows above the peaks while the corresponding Δ's are illustrated by the arrows in the left-hand-side of the figure. Once the width of the peak is known, an energy E_4 can be assigned to its low energy edge and the thickness can then be calculated with our method using in Eq. (9) the kinematic factor for scattering from the film, instead of K_s. The tables of ranges of Ref. [13] were used in these calculations. The results, presented in column 6 of Table II, agree reasonably well with our previous values, shown in column 2 of the same table. Although the same type of analysis could in principle be applied to the Ag/Ta targets, where the Ag-peak appeared superimposed to the Ta-background, larger errors could be expected here because of the small ratio of peak to background areas. For the Al/Ta targets, on the other hand, no Al-peak was resolved at all.

6. CONCLUDING REMARKS

Based on measurements of the global change in energy of particles backscattered from surface atoms of a substrate, with and without a film, a general method is described which uses the known techniques of backscattering spectrometry to determine the thickness of

thin films deposited on thick substrates. As opposed to the usual method, where backscattering from film atoms is considered, this method is not limited to the case of high–Z films on lower–Z substrates. By using a formulation in terms of ranges rather than stopping powers, two analytic approximations are derived by assuming simple linearity relations for the dependence of range with energy. A third analytic approximation using parabolic relations is also discussed. A fast computer program is developed which typically requires only two iterations to calculate the thickness with high accuracy. No random guess is involved in this calculation.

In order to discuss the method, theoretical calculations are performed for hypothetical carbon projectiles and silver targets on Al, Fe and Ta substrates. The piecewise linear approximation gives good results (within less than 3%) for all analyzed cases, but it works better (within less than 0.8%) for the heaviest substrate. The simple linear approximation, on the other hand, is good only for the heaviest substrate, where it gives the same results than the piecewise linear approximation. As for the piecewise parabolic approximation, it gives results which are within 1% for all analyzed cases. Recommendations concerning the choice of target orientation and scattering angle are also discussed.

In order to get experimental support for the method, fourteen targets were measured under different conditions. The method gives generally good results but the associated experimental errors are smaller for heavier substrates. In particular, for substrates with a larger atomic mass than that of the film, where other simple methods don't work at all, the present method can give excellent results.

The main ingredients of the method are a precise determination of the energy change and the use of appropriate data for energy loss calculations. The criterium used in the method for determining the energy change was indirectly checked by comparing with results obtained from a simulation using full dynamic calculations. On the other hand, the use of different energy loss data tables gave consistent results, indicating at most a small effect, upon the method, of the existing uncertainties in such data for the analyzed target materials. For the case of substrates with a lighter atomic mass than the target, a comparison was made with a well known method based on the width of the corresponding scattering peak, obtaining again consistent results.

By a proper choice of the projectile, its energy, the target orientation and the scattering angle, the experimental uncertainties associated with the method can be usually reduced. If precise goniometers (not available in our lab) are used to measure the angles and good care is taken of minimizing gain drifts in the amplifiers, the experimental uncertainties could be brought down to less than 1% if uncertainties in the range data are disregarded. A wide range of target materials and thicknesses can be analyzed with this method, the main limitations being related with the high projectile energies required to measure the thicker targets and the need to have a sizeable ratio of projectile energy-loss to system resolution in order to get acceptable uncertainties.

REFERENCES

1. W-K. Chu, J.W. Mayer and M-A. Nicolet, *Backscattering Spectrometry*, Academic Press (1978).
2. Tsyn-Tyan Yang and Jen-Chang Chou, *Nucl. Inst. and Meth.* **158** (1979) 493.

3. L.C. Feldman and J.W. Mayer, *Fundamentals of surface and thin film analysis*, North-Holland (1986).
4. R. Pengo, *Nucl. Inst. and Meth.* **B56/57** (1991) 933.
5. P.J. Nolan and J.F. Sharpey-Schafer, *Rep. Prog. Phys.* **42** (1979) 1.
6. E.F. Aguilera, Ph.D. Dissertation, University of Notre Dame (1985).
7. E.F. Aguilera, J.J. Kolata, P.A. DeYoung, and J.J. Vega, *Phys. Rev.* **C33** (1986) 1961.
8. G. Dollinger, T. Faestermann and P. Maier-Komor, *Nucl. Inst. and Meth.* **B64** (1992) 422; G. Dollinger, M. Boulouednine T. Faestermann and P. Maier-Komor, *Nucl. Inst. and Meth.* **B79** (1993) 513; *Nucl. Inst. Meth.* **A334** (1993) 187.
9. V. Rigato and G. Della Mea, *Nucl. Inst. Meth.* **A334** (1993) 203.
10. *Ion Beam Handbook for Material Analysis*, eds. J.W. Mayer and E. Rimini, Academic Press, New York (1975).
11. L.R. Doolittle, *Nucl. Inst. Meth.* **B9**, (1985) 344; *Nucl. Inst. Meth.* **B15**, (1986) 227.
12. M.R. Weller, M.H. Mendenhall, P.C. Haubert, M. Dobeli, and T.A. Tombrello, in *Proc. High Energy and Heavy Ion Beams in Materials analysis Workshop*, Eds. J.R. Tesmer, C.J. Maggiore, M. Nastasi, J.C. Barbour and J.W. Mayer, *Materials Research Society* (1990) 139.
13. L.C. Northcliffe and R.F. Schilling, *Nuclear Data Tables* **A7** (1970) 233.
14. R. Burden and D. Faires, *Numerical Analysis*, PWS, Boston, USA (1985).
15. J.F. Ziegler, J.P. Biersack and U. Littmark, *The Stopping and Range of Ions in Solids*, Vol. 1, Pergamon Press (1985).